

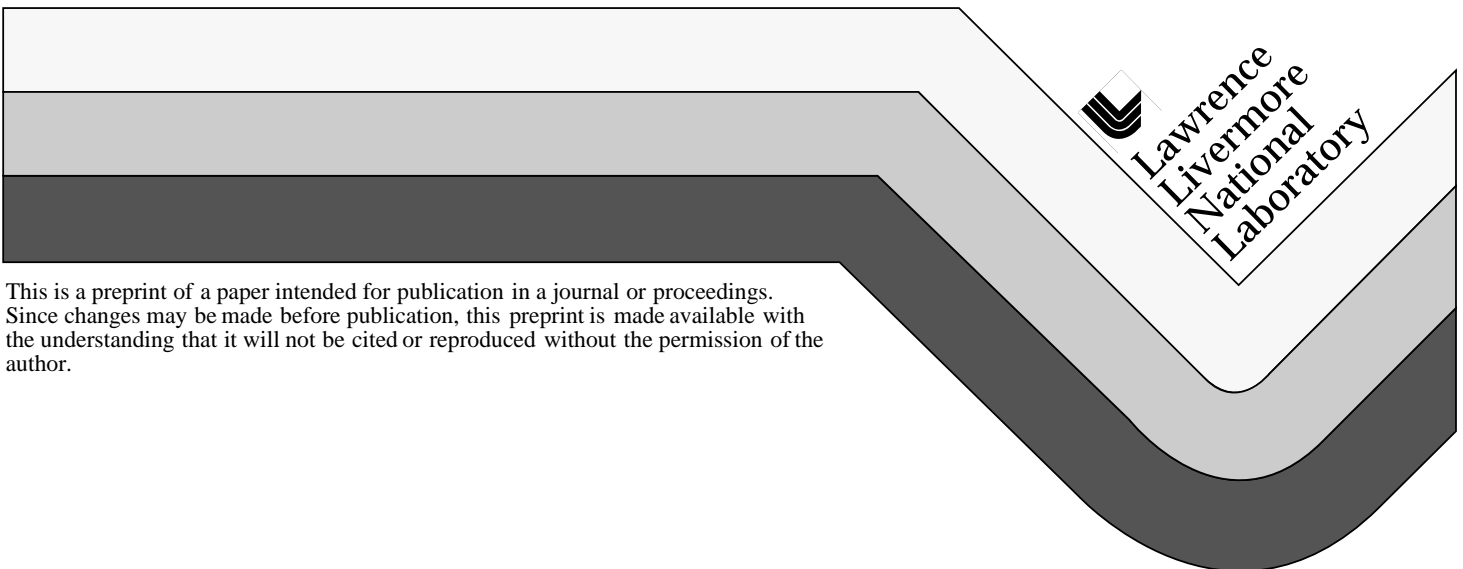
UCRL-JC-134523
PREPRINT

A Strength and Damage Model for Rock Under Dynamic Loading

O.Y. Vorobiev
T.H. Antoun
I.N. Lomov
L.A. Glenn

This paper was prepared for submittal to the
American Physical Society
11th Topical Conference on Shock Compression of Condensed Matter
Snowbird, UT
June 27-July 2, 1999

June 14, 1999



This is a preprint of a paper intended for publication in a journal or proceedings.
Since changes may be made before publication, this preprint is made available with
the understanding that it will not be cited or reproduced without the permission of the
author.

DISCLAIMER

This document was prepared as an account of work sponsored by an agency of the United States Government. Neither the United States Government nor the University of California nor any of their employees, makes any warranty, express or implied, or assumes any legal liability or responsibility for the accuracy, completeness, or usefulness of any information, apparatus, product, or process disclosed, or represents that its use would not infringe privately owned rights. Reference herein to any specific commercial product, process, or service by trade name, trademark, manufacturer, or otherwise, does not necessarily constitute or imply its endorsement, recommendation, or favoring by the United States Government or the University of California. The views and opinions of authors expressed herein do not necessarily state or reflect those of the United States Government or the University of California, and shall not be used for advertising or product endorsement purposes.

A STRENGTH AND DAMAGE MODEL FOR ROCK UNDER DYNAMIC LOADING

Oleg Yu. Vorobiev, Tarabay H. Antoun, Ilya N. Lomov, Lewis A. Glenn

Lawrence Livermore National Laboratory, Geophysics@Global Security Division, Livermore, CA 94550

Abstract. A thermodynamically consistent strength and failure model for granite under dynamic loading has been developed and evaluated. The model agrees with static strength measurements and describes the effects of pressure hardening, bulking, porous compaction, porous dilation, tensile failure, and failure under compression due to distortional deformations. This paper briefly describes the model and the sensitivity of the simulated response to variations in the model parameters and in the inelastic deformation processes used in different simulations. 1D simulations of an underground explosion in granite are used in the sensitivity study.

INTRODUCTION

Modeling the dynamic response of rock materials is a challenging area of research. Since most strength measurements in rock materials are performed for intact samples under static conditions, the models based on these data should account for possible scale and rate effects when being applied to simulation of the dynamic response of large scale rock masses. Unlike intact rock samples, rock masses may contain discontinuities which may reduce the strength and cause anisotropic behavior.

We assume that the material is isotropic for the problem of interest and apply the mathematical structure of plasticity theory to capture the basic features of the mechanical response of geological materials. We use experimental data obtained under static conditions to calibrate the model and fit rate-dependent model parameters to describe the dynamic measurements in spherical shock waves.

CONSTITUTIVE EQUATIONS

To model the dynamic response of material to shock wave loading, the system of equations

representing the mass, momentum and energy conservation laws is supplemented by the following equation for the unimodular tensor of elastic distortional deformation \mathbf{B} [1].

$$\dot{\mathbf{B}} = \mathbf{L}\mathbf{B} + \mathbf{B}\mathbf{L}^T - \frac{2}{3}(\mathbf{D} \cdot \mathbf{I})\mathbf{B} - \mathbf{A}_p; \quad (1)$$

$$\mathbf{A}_p = \Gamma_p \left[\mathbf{B} - \frac{3\mathbf{I}}{\mathbf{B}^{-1} \cdot \mathbf{I}} \right]$$

Using \mathbf{B} , the deviatoric stress \mathbf{T}' can be expressed as $\mathbf{T}' = G \frac{\rho(1-\Phi)}{\rho_0} (\mathbf{B} - \frac{1}{3}(\mathbf{B} \cdot \mathbf{I}))$,

where G is the shear modulus, ρ_0 and ρ are the initial and the current density and Φ is the reference porosity.

In Eq. (1), Γ_p specifies the plastic response of the material and is taken to be a function of the von Mises effective stress σ_e and the yield strength Y [2]:

$$\Gamma_p = \Gamma_{p0} \left(\frac{3G}{\sigma_e} \right) \left(\frac{\langle \sigma_e - Y \rangle}{Y_0} \right)^2 \quad (2)$$

The conservation laws are integrated numerically using the second order Godunov scheme. Eq. (1) is integrated using the velocity gradient tensor \mathbf{L} and its symmetric part, \mathbf{D} , approximated by solving the Riemann problem.

More details about the numerical algorithm can be found in [3].

STRENGTH OF MATERIAL

The physical phenomena that influence the yield strength Y are accounted for by assuming a simple multiplicative form with Y being given by [1]

$$Y = Y_0 F_1(\epsilon_p) F_2(p) F_3(\Omega) F_4(\beta) F_5(\theta) \quad (3)$$

The functions F_i in (3) represent hardening effects due to plastic strain (F_1) and pressure sensitivity (F_2), as well as softening due to distortional deformation damage (F_3) and melting (F_5). F_4 is a function of the Lode angle.

In our study of spherical wave propagation in granite we have found that the response of the material is most sensitive to the first three functions in Eq. (3). The analytical forms of the functions F_i are described in [1]. The damage parameter, Ω , used in the function (F_3) is evaluated using the relation

$$d\Omega = \frac{\langle T_{\max} - T_{th} \rangle dt}{\tau_{dam} Y_0} \quad \text{if } \epsilon_p > \epsilon_p^* \quad (4)$$

where T_{\max} is the most compressive principal stress, T_{th} is the threshold stress for damage growth, and τ_{dam} is a characteristic time for damage. The onset of damage is controlled by a critical plastic strain parameter, ϵ_p^* , which can be chosen to describe the failure surface measured in static experiments [4] (see Fig.1).

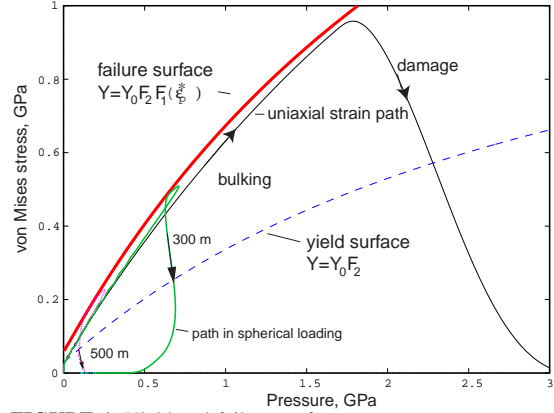


FIGURE 1. Yield and failure surface.

The divergent flow of spherical shock loading leads to a wide variety of stress states in contrast to plane waves, where the locus of all states is represented by a straight line in yield-pressure space.

POROUS COMPACTION AND BULKING

The equations used to describe the evolution of porosity are given in [1]. Here we only provide a brief description.

To describe the increase of porosity due to distortional deformation (bulking), the following equation is used:

$$\dot{\phi} = (1 - \phi) \frac{m_d(\phi, p) Q}{P}, \quad \phi_{\max} < \phi^*, \quad \phi_{\min} < \alpha \Phi \quad (5)$$

where Q is the rate of dissipation given by

$$Q = \frac{1}{2} \frac{\rho(1 - \Phi)}{\rho_0} \Gamma_p G(\mathbf{B}' \cdot \mathbf{B}'), \quad (6)$$

\mathbf{B}' is the deviator of \mathbf{B} and ϕ_{\max} , ϕ_{\min} are the maximum and the minimum porosities for all times. The maximum bulking porosity is specified by ϕ^* . The rate of bulking m_d is chosen to be a linear function of porosity and pressure as

$$m_d = m_{d0} + a_1 \phi + a_2 P, \quad 0 < m_d < 1 \quad (7)$$

Figure 2 shows how well it is possible to fit this model to laboratory bulking data.

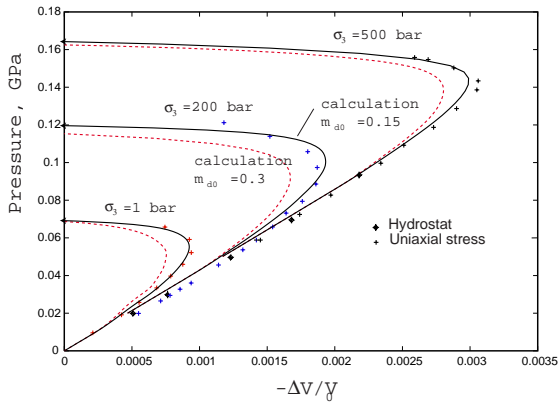


FIGURE 2. Volume strain as a function of pressure for granodiorite during uniaxial stress loading at several confining pressures. The points are experimental data [4], the solid and dashed lines are calculations with different values for m_{d0} .

According to Eq. (5), bulking is not allowed until the porosity is reduced in compaction to a fraction of the initial porosity (which is typically 0.1-1% of the initial porosity). Eq.(5) is derived from the entropy dissipation condition in order to satisfy the second law of thermodynamics when porosity increases at positive pressure.

EFFECT OF MODEL PARAMETERS

To study the effect of the model parameters on the material response we have simulated an explosion in granite with different constant yield strength values. The source was modeled using ideal gas with granite density. We used a Mie-Grüneisen EOS for the granite. A more general tabular EOS was subsequently employed and produced similar results. The simulation results in Fig.3 show that using a constant yield strength we cannot describe the negative phase of the pulse (so-called rebound). It has been shown in previous research that yield strength degradation is required to obtain a deep and wide rebound signal [5]. Pressure hardening makes the pulse even more narrow unless we introduce damage.

Figure 4 shows several velocity waveforms calculated using the current model. The numbers on the plot designate the different phases of the pulse. During phase 1, the material is compacted in shock loading. The pressure, and correspondingly the yield strength are increasing

depending on the slope of the compaction curve. Bulking takes place after porosity drops to a small fraction of the initial porosity in compaction, and only if the von Mises stress has reached the onset of yield surface. Phase 2 begins when the pressure starts decreasing after reaching a maximum value. Phase 3 starts after the material is fully damaged. This phase may not happen if the von Mises stress in loading does not reach the failure surface.

Our simulations show that bulking has a large effect on the peak stress (see Fig.5). The calculation without bulking gives 3-4 times less peak stress. Damage does not change peak stress attenuation significantly, but it appears to have a significant effect on the pulse width and displacement. Hydrodynamic theory [6] agrees with calculations up to pressures of a few GPa and deviates in the region where material strength is important.

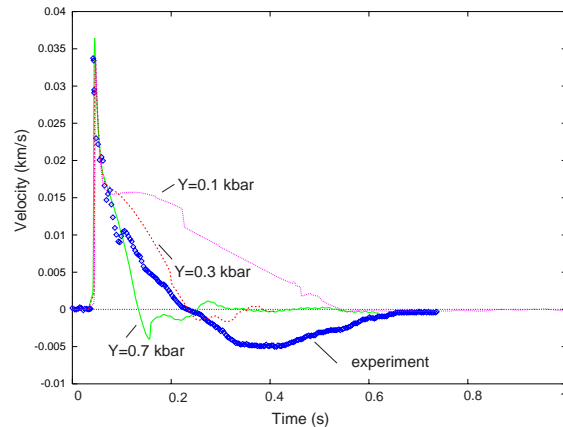


FIGURE 3. Velocity histories calculated for an explosion in granite at 204 m with constant yield strength in comparison with the experimental data.

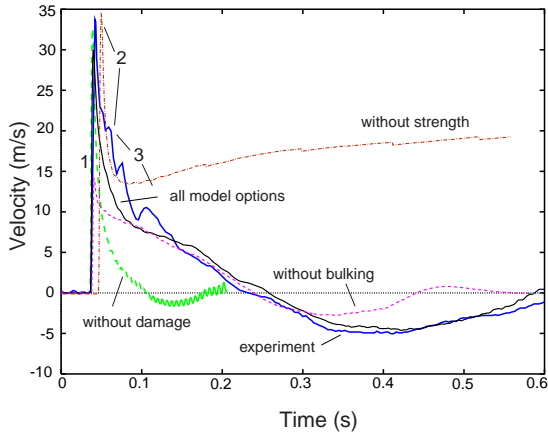


FIGURE 4. Velocity histories calculated with different model options in comparison with experimental profile (bold line).

Since the damage model developed is scale-dependent, damage will not happen if the characteristic time of the problem is much less than τ_{dam} which is of the order of 10 ms. This is illustrated in Fig.6 where scaled velocity histories are shown. The shape of the velocity profile becomes more narrow when the scale of the problem is reduced. That explains why the calculated scaled peak displacement is less for explosions with smaller energy yields as shown in Fig.7.

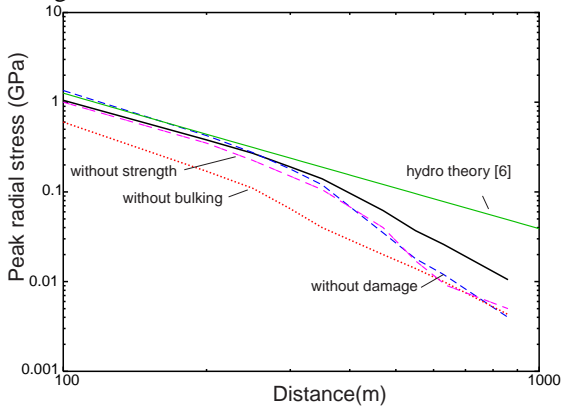


FIGURE 5. The peak radial stress attenuation with distance.

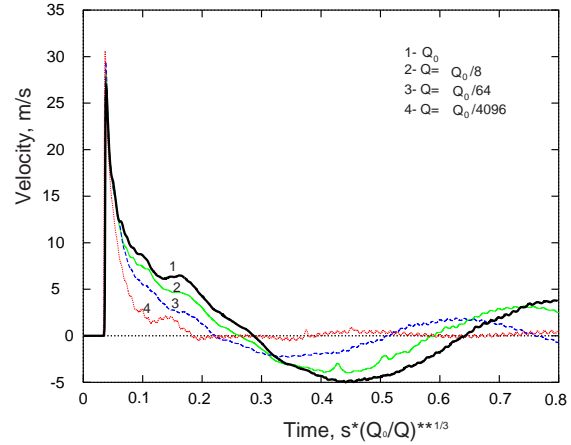


FIGURE 6. Velocity profiles calculated at the same scaled range $50 m/kt^{1/3}$ for explosions with different energy yields.

CONCLUSIONS

A new scale-dependent strength and damage model has been developed which gives good agreement with both static tests and dynamic measurements of large scale motion caused by underground explosions. The model includes the effects of bulking, pressure hardening and damage due to distortional deformations which are found to be important to simulate the material response, especially in spherical loading.

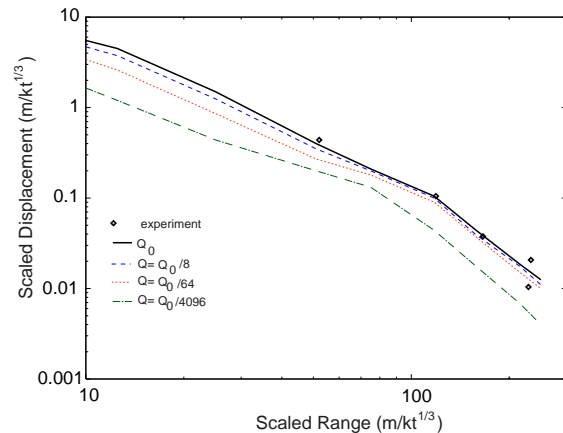


FIGURE 7. Attenuation of scaled peak displacement calculated for different yields. The points are experimental data [7].

ACKNOWLEDGMENTS

Work performed under the auspices of the U. S. Department of Energy by the Lawrence Livermore National Laboratory under Contract W-7405-ENG-48.

REFERENCES

1. Rubin, M.B, Vorobiev, O.Yu., Glenn, L.A., accepted for publication in *Int. J. Solids and Structures* (1999)
2. Swegle, J. W. and Grady, D. E., *J. Appl. Phys.*, **58**,692-701 (1985)
3. Vorobiev, O. Yu, Glenn, L. A., Rubin, M. B., *Simulation of the dynamic response of porous elastic-viscoplastic materials*, to be published
4. Schock, R. N., Heard, H. C., and Stephens, D. R., *J. Geophys. Res.*, **78**(36), 5922-5941 (1973).
5. Stevens, J. L., Rimer, N., and Day, S. M., "Constraints on Modeling of Underground Explosions in Granite," Report SSS-R-87-8312, S-Cubed division, Maxwell Labs (1986).
6. Lamb, F. K., Callen, B. W., Sullivan, J. D., *J Geophys. Res.*, **97**, 515-535 (1992)
7. Perret, W.R., "Free Field Ground Motion in Granite", Report No. POR-4001, Sandia Laboratory, Albuquerque, New Mexico (1968)